Effect of process parameters on synthesis of aluminum nitride powder prepared by chemical vapor deposition

MOO-CHIN WANG
Department of Mechanical Engineering, National Kaohsiung University of Applied Sciences, 415 Chien-Kung Road, Kaohsiung, 80782, Taiwan

MING-SUNG TSAI, NAN-CHUNG WU
Department of Materials Science and Engineering, National Cheng Kung University, 1 Ta-Hsueh Road, Tainan, 70101, Taiwan
E-mail: n5884105@sparc1.cc.ncku.edu.tw

Ultrafine aluminum nitride (AlN) powders were obtained by the chemical vapor deposition (CVD) process via the $AlCl_3$-N_2-NH_3 system operated at various temperatures and different mixing modes of $AlCl_3$ and NH_3 gases. X-ray diffraction (XRD), Fourier transform infrared spectroscope (FTIR), transmission electron microscope (TEM) and electron diffraction (ED) were utilized to study the effect of process parameters on the synthesis and characterization of the AlN powders. It had been shown that all of the obtained powders were exclusively identified to be the single phase AlN and were indifferent to the different mixing modes $AlCl_3$ and NH_3 gases. The yield of synthesized AlN powder was affected by the entries mixing position of the reacting gases of $AlCl_3$ and NH_3. The yield increased from 13% to 82% where the mixed position was shifted from the front edge to middle point of the quartz tube. On the other hand, the yield increased from 5% to 82% as the reaction temperature increased from 600°C to 1050°C. The morphology of the AlN powders was affected by the diameter of a feeding nozzle and mixing mode of $AlCl_3$ and NH_3 gases.
© *2001 Kluwer Academic Publishers*

1. Introduction

A high-purity aluminum nitride (AlN) powder is very useful for the fabrication of ceramic bodies for advanced electronics applications because it is a chemically inert compound with high thermal conductivity and high electrical resistivity [1]. The thermal conductivity of AlN ceramics is strongly influenced by its chemical purity and density, while the theoretical value is predicted to be $319 W/m \cdot K$ at room temperature [2]. Slack [3] has reported that phonon scattering in the oxygen-doped sample is caused by the aluminum vacancies which are dissolved in the AlN matrix and hence the thermal conductivity decreases as the oxygen content increases. In addition, the thermal expansion coefficient of AlN at room temperature is 4.3×10^{-6}/K, near that of Si [4]; and the dielectric constant at 1 MHz and room temperature is 8.9 [4]. On the other hand, AlN powder can be pressureless sintered with additives to theoretical density [5].

In general, electronics substrate and packaging applications are the most stringent and require powders which can be pressureless sintered with additives to manufacture flawless, fully dense AlN components of high thermal conductivity and uniform light color [5]. But AlN powder does not occur naturally; therefore, it must be synthesized by nitridation. Various batch methods containing the carbothermal reduction of Al_2O_3, direct nitration of aluminum and plasma process have been reported [5–15]. These batch methods are disadvantageous for continuous powder production.

In recent years, the preparation of AlN powder by a continuous process using the chemical vapor phase of $AlCl_3$ with NH_3 and varying the reaction temperature, the molar mixture of starting materials and the reaction assembly have been reported [16–19]. Synthesis of ceramic powders by gas phase materials is advantageous to produce high-purity fine powders with uniform particle size, because powders are formed homogeneously and it is relatively easy to control the nucleation process [16].

In the present study, single phase AlN powders were obtained by the chemical vapor deposition (CVD) process. The AlN powders formed were characterized by X-ray diffraction (XRD), Fourier transform infrared spectroscope (FTIR), transmission electron microscope (TEM) and electron diffraction (ED). The purposes of this investigation were to evaluate the effect of entry/mixing of the reacting gases of $AlCl_3$ and NH_3 on the synthesis of AlN powders, the morphology of AlN powders, the yield of AlN powders synthesis and the characterization of the AlN powders.

2. Experimenial procedure
2.1. Powder preparation
The raw materials of commercial grade were used in the experiment. A schematic diagram of the experimental equipment is shown in Fig. 1. This system consisted of a raw materials transport system, a tubular synthesis reactor, a vacuum system, and a powder collection system. Four different feeding tube assemblies as shown in Fig. 2 were tested in order to investigate its effect on the AlN deposition.

The temperature distribution of the reaction chamber for AlN powders synthesis is shown in Fig. 3. The reaction temperature below 600°C cannot yield the crystalline AlN powders, hence it is defined the high temperature zone as the reaction chamber temperature greater than 600°C; otherwise, below 600°C and outside of the reactor as defined the low temperature zone [20].

Before synthesis, the quartz tube reactor (42.0 mm inner diameter and 700.0 mm long) was first preheated and held at 250°C; subsequently evacuated to 0.8 torr by using rotary and oil-diffusion pumps, and purged with nitrogen gas three times. $AlCl_3$ vapor with the pressure of 760 torr was formed by heating solid $AlCl_3$ (purity 98%, supplied by Wako Pure Chemical Industries, Japan) to 180°C. The $AlCl_3$ vapor was then carried to the reactor chamber by nitrogen carries gas stream (purity 99.99%, supplied by Lien Hwa Air Co., Taiwan) at a flow rate of 200 cm^3/min. The NH_3 was fed into

Figure 3 The temperature distribution of the reaction chamber for AlN powders synthesis, the center of quartz tube as zero.

the reactor chamber at a flow rate of 200 cm^3/min through another tube and reacted with gaseous $AlCl_3$ at various temperatures. The reaction temperature was measured by a Pt/Pt-Rh thermocouple positioned immediately above the inlet at the middle zone of the quartz tube. The resulting powders were collected in a flask.

2.2. Characterization
The crystal structure of the powders was examined using an X-ray diffrectormeter with Cu K_α radiation and Ni filter operated at 30 kV, 200 mA and a scanning rate of 0.25°/min (Model Rad IIA, Rigaku, Tokyo).

The morphology of the powders was examined by transmission electron microscope (TEM, H700H, Hitachi). Quantitative analysis for Si, Fe, Mg, and Ca was obtained by an inductively coupled plasma method. The nitrogen and oxygen analyses were performed using a TC136 LECO EF100 electrode furnace and associated analyzer.

FTIR absorption spectra were obtained by processing on an optical bench of the standard Nicolet's system 800 Fourier transform imfrared spectrometer and a spectral resolution of 4 cm^{-1} was chosen. Each test sample was mixed with KBr (1wt% of the former), and was pressed into 200 mg-pellets of 13 mm diameter for infrared absorption spectra at a frequency range of 400–4000 cm^{-1}. The composite spectrum for each sample represented an average of 64 scans, normalized to the spectrum of the blank KBr pellet.
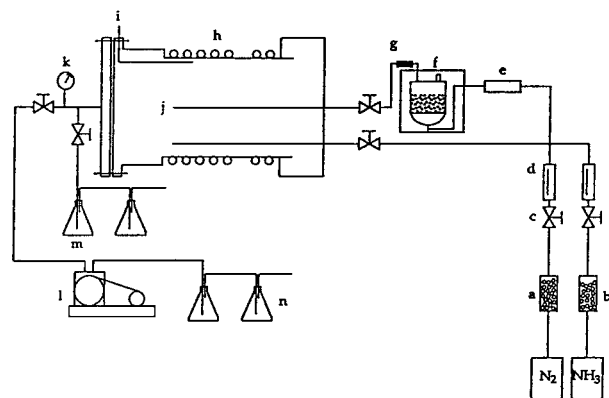
Figure 1 Schematic diagram of the experimental apparatus for synthesized AlN powders. (a) phosphoric analydride, (b) sodium hydrate particle, (c) ball valve, (d) flowmeter, (e) spongy titanium, (f) aluminum chloride (purity 98%), (g) ribbon heater, (h) $MoSi_2$ heater, (i) thermocouple, (j) quartz tube reactor, (k) pressure gage, (l) vacuum pump, (m) powder collection flask, (n) NaOH solution.
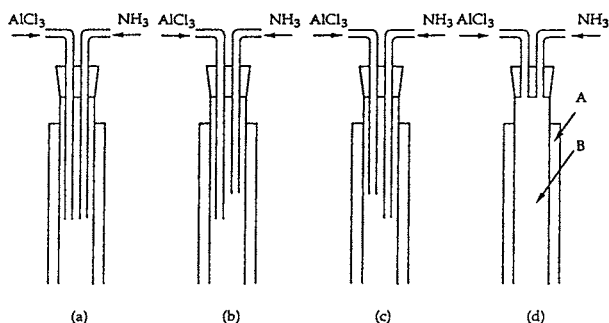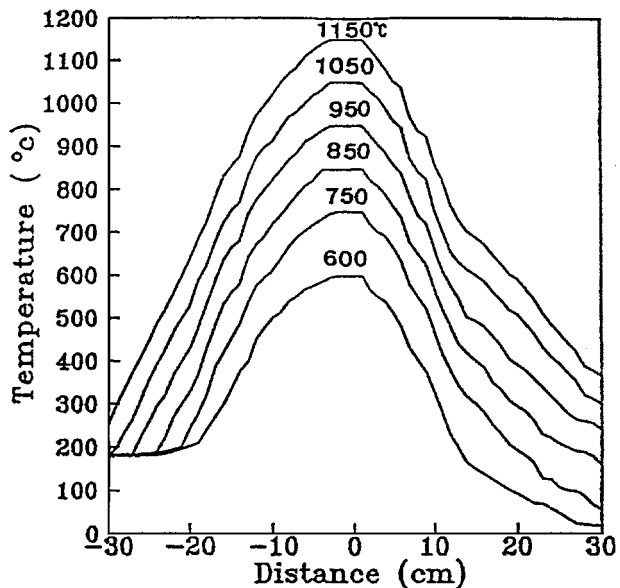
Figure 2 Section of the CVD reactor showing the different position (a. b. c and d) of the feeding nozzles for $AlCl_3$ and NH_3: (A) furnace, (B) reactor quartz tube.

3. Results and discussion
3.1. Effect of mixing mode on the powder synthesized
Typical XRD patterns of the AlN powders collected in the higher temperature zone of the CVD reactor at 1050°C with different mixing modes as represented in
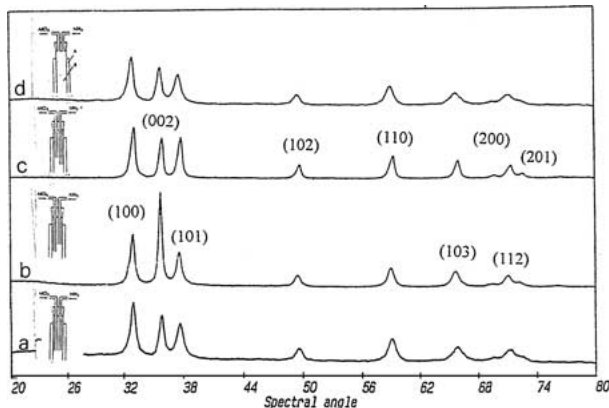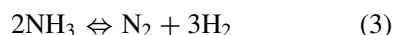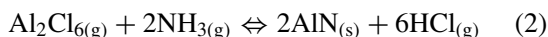
Figure 4 The XRD patterns of the AlN powders collected in the CVD reactor at 1050°C and different mixing modes as represented in Fig. 2.

Fig. 2 are shown in Fig. 4. Only AlN [21] was detected and no indication of $AlCl_3$ was found from the powders, irrespective of the difference in mixing shown in Fig. 2 corresponding to the experimental results of Kimura *et al*. [22] who observed the formation of crystalline AlN powders even at the temperature as low as 600°C. The crystallinity of these powders was almost the same as those collected from the higher temperature zone of the CVD reactor at 1050°C except for the case of Fig. 2b. The intensity of reflection (202) is greater than that of (100), being presumed as caused by the variance of the feeding condition that induces the difference in concentration, temperature and pressure and consequently, the crystal growth direction is changed.

In 1950's, the reaction system of $AlCl_3/NH_3$ has been investigated in order to produce either pure AlN films [23] or AlN powders [17, 22]. Riedel and Gaude [18] pointed out that the thermodynamic calculations can predict that the formation of AlN via the gas phases according to Equation 1 or 2 is difficult because the decomposition reaction of ammonia into elements [Equation 3] occurs at temperature above 127°C and 0.1 MPa pressure.

$$AlCl_{3(g)} + NH_{3(g)} \Leftrightarrow AlN_{(s)} + 3HCl_{(g)} \qquad (1)$$

$$Al_2Cl_{6(g)} + 2NH_{3(g)} \Leftrightarrow 2AlN_{(s)} + 6HCl_{(g)} \qquad (2)$$

$$2NH_3 \Leftrightarrow N_2 + 3H_2 \qquad (3)$$

The reaction represented by Equation 2 also must be taken into account in the system of $AlCl_3/NH_3$, since at the sublimation temperature (180°C) $AlCl_3$ is present in the form of its dimer Al_2Cl_6 in the gas phase. The formation of monomeric $AlCl_3$ gas species is observed at temperature exceeding 800°C [17].

Although Riedel *et al*. [18] proposed above explanation, in the present study, amorphous AlN was obtained at a temperature below 600°C with NH_4Cl as a by-product. This result was discussed in our previous paper [20]. Hence, at lower reaction temperatures, AlN can also be formed via the following reaction [16]

$$AlCl_{3(g)} + 4NH_{3(g)} \Leftrightarrow AlN_{(s)} + 3NH_4Cl_{(s)} \qquad (4)$$

Ammonium chloride can also be formed below about 250°C via the reaction [16]

$$NH_{3(g)} + HCl_{(g)} \Leftrightarrow NH_4Cl_{(s)} \qquad (5)$$

In the present study, gas reactants of $AlCl_3$ and NH_3 were mixed in the cold zone of the reactor (below 200°C), with the mixing mode shown in Fig. 2d, and amorphous AlN coating on the inside wall of the quartz tube and hard agglomerates of AlN particles grown on the surface of the AlN film were obtained. Since the temperature in the mixing zone is so low, none of that AlN powders are formed there and the film thickness at the front of the quartz tube increases. If the effective reaction temperature can not be increased and the chemical reaction rate decreases, then the concentration of the precursor for nuclei formation decreases, because the supersaturation is insufficient. As the particle formation is very sensitive to supersaturation degree, the yield of the powder formation suddenly decreases with increasing film coating on the quartz tube wall.

Both feeding nozzles shown in Fig. 2d were located in the cold zone of the CVD reactor at 1050°C. The reaction of $AlCl_3$ with NH_3 as described by Equation 4 has to be considered. The formation of Lewis acid -Lewis base adduct compounds prior to the decomposition into AlN according to

$$AlCl_3 + xNH_3 \Leftrightarrow AlCl_3 \cdot xNH_3 \qquad (6)$$

has been proved by characterizing the intermediate reaction product. These adduct compounds decompose at temperature above 700°C to form AlN and HCl [16]. Nickel *et al*. [24] have pointed out that one of the problems of this approach is that a large fraction of AlN formed in the decomposition of this adduct ($AlCl_3 \cdot xNH_3$) is in the form of a coating inside the quartz tube. These AlN powders formed through this adduct are amorphous.

3.2. Effect of entry/mixing position on the AlN powders morphology

Fig. 5 shows the TEM micrograph of AlN powder synthesized at 1050°C which NH_3 and N_2 at the same flow rate 200 cm³/min for different feeding modes as represented in Fig. 2. Three different types of powders were observed in Fig. 5. The particles observed by TEM are regarded as primary particles which are composed of more crystallites and become coarser when the feeding position shifts from the middle zone to the front edge of the quartz tube. When NH_3 and $AlCl_3$ mix in the middle zone of the quartz tube the round particles are produced as shown in Fig. 5a. The particle size seems to be uniform. These primary particles are linked together to form many agglomerates. During feeding the nozzles of $AlCl_3$ and NH_3 were located at the middle zone 20 cm from the front edge.
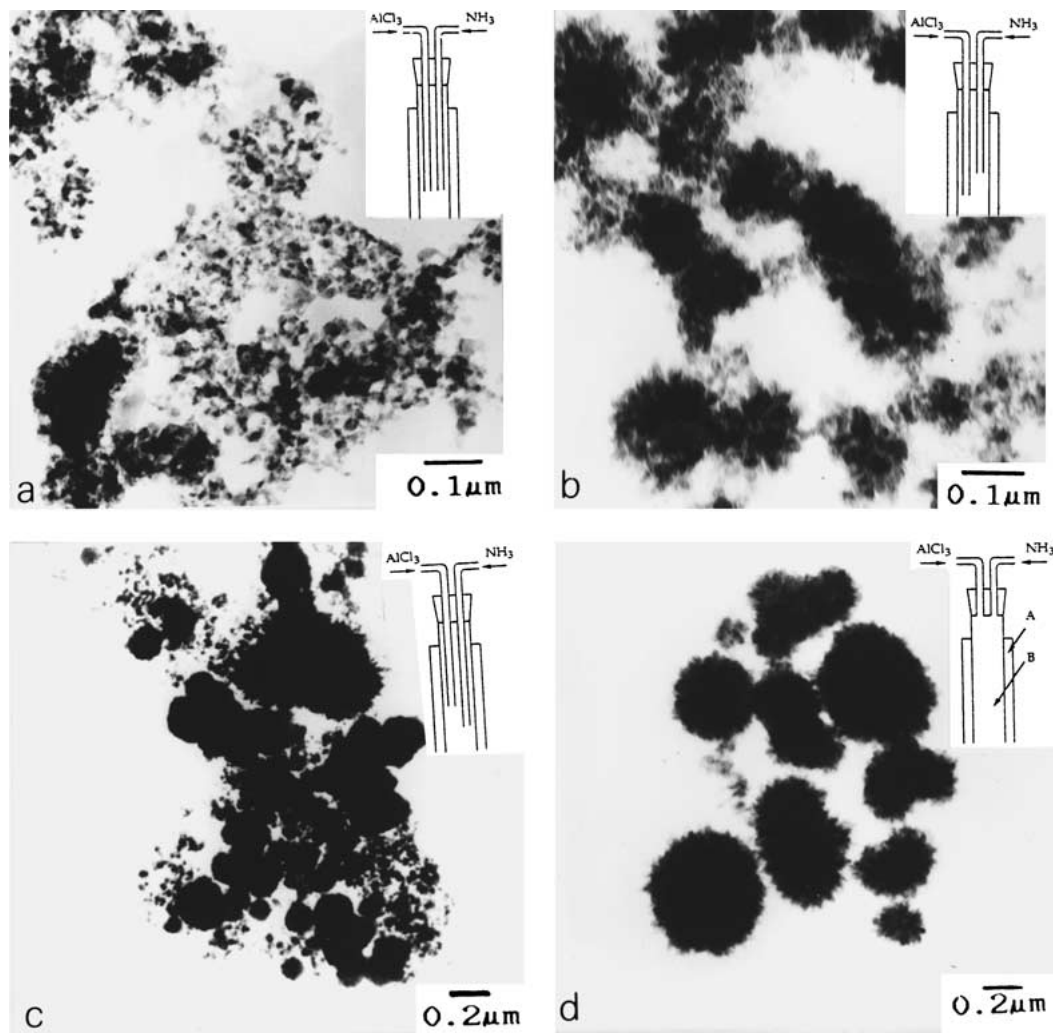
Figure 5 The TEM micrograph of the AlN powder synthesized at 1050°C for NH_3 and N_2 at same flow rate 200 cm^3/min and for different mixing mode as represented in Fig. 2.

The shape of primary particles was polyhedral and the size was less than 0.1 μm. Since primary particle size was greater than that of Fig. 5a, the crystal growth of AlN must have occurred. When the feeding nozzles of NH_3 and $AlCl_3$ were that shown in Fig. 2c, the shape of primary particles were polyhedral and partial hexagonal and the crystal growth of the resulting AlN was promoted. Both gas species, $AlCl_3$ and NH_3, were mixed in the cold zone of the quartz tube (below 200°C) with Fig. 2d mode. The morphology of the obtained particles with radial growth is shown in Fig. 5d. From Fig. 5, it is concluded that when both feeding nozzles were located in the hot zone of the CVD reactor at 1050°C are such that represented in Fig. 2, nuclei formation is enhanced and fine particles production are produced.

When the temperature of the CVD reactor was at 1050°C and the feeding located in the middle zone was such that represented in Fig. 2a, the TEM micrograph of the resulting powders prepared with the different diameter of $AlCl_3/N_2$ feeding nozzle is shown in Fig. 6. It can be observed that as the inlet diameter of the $AlCl_3$ feeding nozzle increases from 6 to 9 mm, the particle size of the resulting AlN powders tends to become coarser. This phenomenon leads to the conclusion that for small nozzle, the heating rate of the reactant gas,

the effective reaction temperature and the rate of nuclei formation are increased in sequence, resulting in finer particles.

3.3. Effect of entry/mixing on the yield of AlN powder

The equilibrium yield, η_{AlN}, of each aluminum compound (aluminum nitride and aluminum chloride) with respect to the initial chloride composition could be determined. The aluminum nitride yield is defined by the ratio [25]

$$\eta_{AlN} = \frac{N_{AlN}}{N_{AlCl_3}} \qquad (7)$$

where N_{AlN} is the number of moles of aluminum nitride formed, and N_{AlCl_3} denotes the number of moles of consumed aluminum chloride.

One of the most important goals in the development of the chemical synthesis process is to obtain a maximum yield of the product. In the present study, most of the product was recovered inside the quartz tube and the flask connected to the outlet of the tube. Powders recovered inside the quartz tube were from the homogeneous nucleation at a given reaction temperature and the ones from the flask were probably a mixture of the
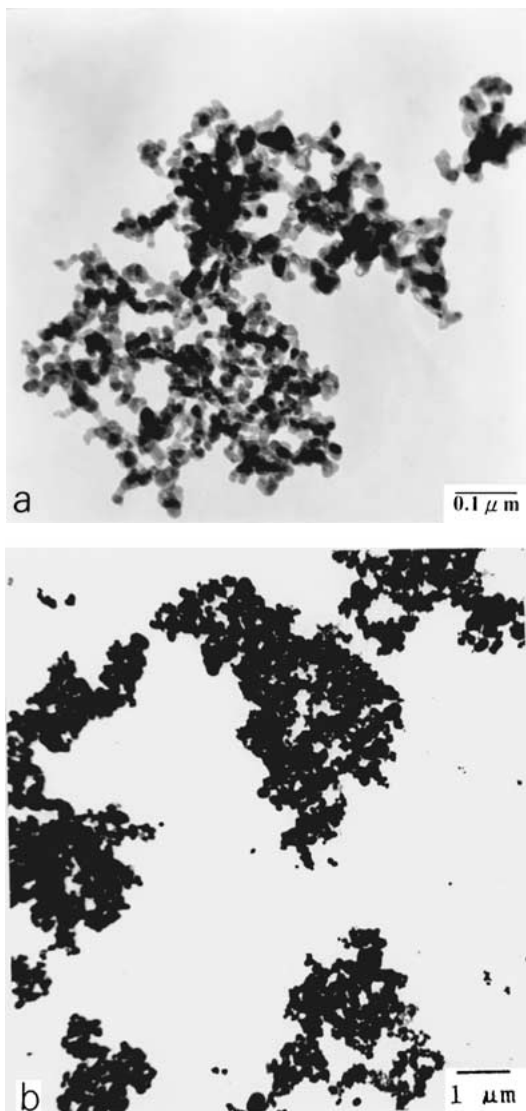
Figure 6 The TEM micrograph of the AlN powders synthesized at 1050°C from the different diameters of $AlCl_3/N_2$ feeding nozzle for NH_3 and N_2 at the same flow rate 200 cm^3/min: (a) 6 mm, (b) 9 mm.

powders carried out of the quartz tube and the powders formed at lower reaction temperatures inside the flask.

For the reaction temperature at 1050°C and the same flow rate of 200 cm^3/min for NH_3 and N_2 with the different feeding modes represented in Fig. 2, the yields of synthesized AlN powders are listed in Table 1. Where both feeding nozzles were located at the front edge of

the quartz tube, the total AlN yields was only 13%. This phenomenon is presumed to be caused by the fact that while the temperature of the middle zone was 1050°C, the reaction temperature was below than 600°C at the front edge of the tube and the gaseous aluminum chloride would not be dissociated into the monomer $AlCl_3$ prior to the reaction with ammonia [18]. Under this condition hard\agglomerated crystalline AlN was obtained. In the present study, only when both feeding nozzles located at the front edge was had this result. Peuleau *et al*. [25] pointed out that the yields of aluminum nitride and aluminum halides are a function of the trihalide vapor pressure and the ammonia vapor pressure. The increase of the yield of aluminum monochloride corresponds to the decrease of the yield of aluminum nitride. The yield of aluminum nitride decreases rapidly at an initial aluminum trihalide vapor pressure higher than 10^{-3} atm during the dissociation of ammonia at equilibrium. The yield of dimers (Al_2Cl_2) is always less than 1% and the yield of aluminum dichloride ($AlCl_2$) is also very low [25].
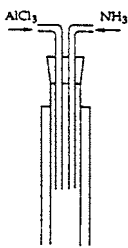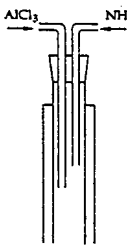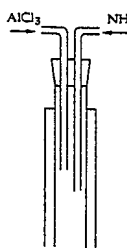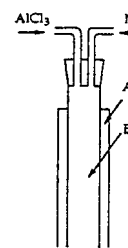
The amount of AlN could be increased up to 82% as the feeding nozzles where shifted from the front edge to the middle zone of the reactor, using Fig. 2a instead of Fig. 2d. According to Peuleau *et al*. [25], the decomposition rate increased when the feeding nozzles shifted from the front edge to the middle zone of the reaction and the effect of the location of the feeding nozzle for $AlCl_3$ was greater than N_2.

Fig. 7 shows the yield of AlN as a function of the reaction temperature at the same folw rate of NH_3 and N_2, 200 cm^3/min, respectively. For the reaction at 600°C, the yield was very low, only 5%. This is probably due to the fact that ammonia dissociates into H_2 and N_2 and not enough active source is available. Nickel *et al*. [24] has pointed out that maximum yield can not be higher than 20% as the ammonia dissociates to N_2 and H_2 by the thermodynamic calculation. At 600°C, the yield was extremely low because the reaction rate was very slow.

3.4. Characterization of AlN powder

The FTIR spectroscopic result for the AlN powders heat treated in the NH_3 atmosphere at various temperatures for 2 h was shown in Fig. 8. The Al-O peak was observed at 460 cm^{-1} after heat treatment. The FTIR

TABLE I The relation between AlN synthesis yield and various mixing modes of NH_3 and $AlCl_3/N_2$

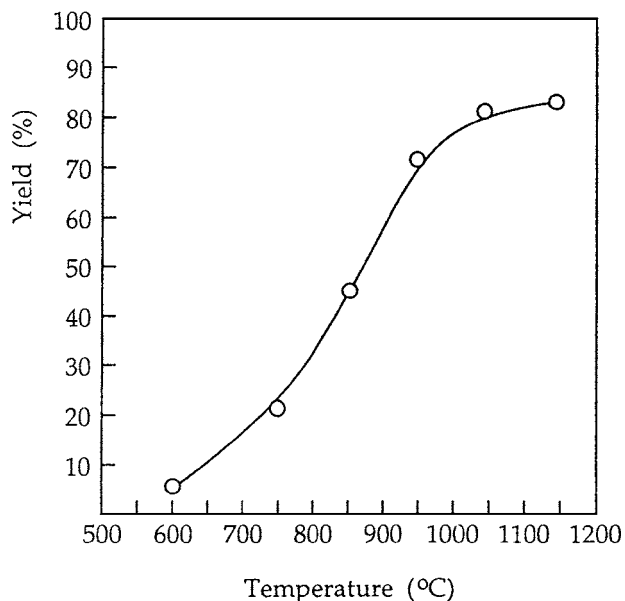|				
Mixing mode				
Yield(%)	82	76	37	13

Figure 7 The relation between AlN synthesis yield and various temperatures for NH_3 and N_2 at the same flow rate 200 cm^3/min.
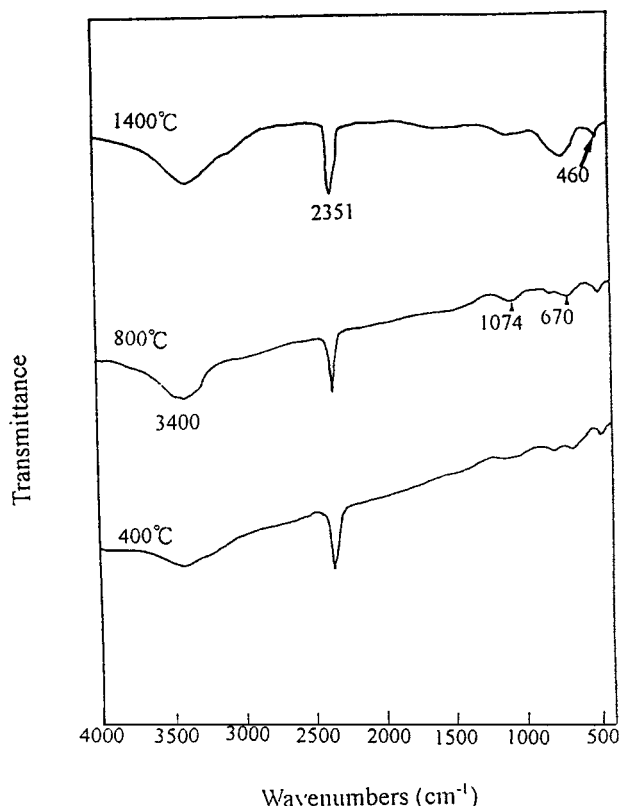

Figure 8 FTIR spectra for the powders obtained after heat treatment at various temperatures.

spectrum shows a broad peak related to Al-N bonds at 670 cm^{-1} [11]. Since NH_3 was used as a nitriding agent, thus the peak appeared at 2351 cm^{-1} might be attributed to the presence of ν (NH_3) in Al-NH_2 [26]. A broad peak related to ν (NH_3) bending variation around 1074 cm^{-1} could be found, and a broad peak centered around 3400 cm^{-1} was due to the presence of O-H or N-H bands [26].

The oxygen and nitrogen contents of AlN powder formed by $AlCl_3$/50%N_2-50%NH_3 and heat-treated at

TABLE II The nitrogen and oxygen atom contents of AlN powders for various heat-treatment atmospheres

Heat treatment atmosphere	Content (wt%)	
	N	O
N_2	17.6	12.9
NH_3	24.8	4.7

TABLE III The contents of trace metallic elements of AlN powders

Metallic element	Content (ppm)
Si	53.8
Fe	5.36
Mg	5.15
Cu	5.80

1200°C under N_2 and NH_3 atmosphere for 2 h are listed in Table II. The presence of oxygen in the powders may be due to the chemisorption of H_2O on the surface of primary particles [18]. This assumption is supported by the results of Fig. 8 where a broad absorption band shows the presence of H_2O appearing in the range 4000–3000 cm^{-1}.

The results of powders were examined by an inductively coupled plasma technique having a detectability for metallic impurity elements as listed in Table III. Most metallic impurity elements are about 5 ppm, except Si content up to 53.8 ppm. Most of the trace impurities in the AlN powders are probably introduced during the conversion of $AlCl_3$ into AlN [27].

4. Conclusions

Ultrafine AlN powders were prepared by the CVD process via the $AlCl_3$-N_2-NH_3 system operated at various temperatures and different mixing modes of $AlCl_3$ and NH_3. The results in the present investigation are summarized as follows:

(1) All of the obtained powders exclusively belong to the same single phase AlN, and are indifferent to the variation of the mixing modes of $AlCl_3$ and NH_3.

(2) The morphology of AlN powders is affected by the mixing mode of $AlCl_3$ and NH_3. When NH_3 and $AlCl_3$ are mixed at the middle zone of the reactor, the shape of the primary particle is polyhedral with size less than 0.1 μm. On the other hand, as the $AlCl_3$ and NH_3 are mixed at the front edge of the reactor, the particle morphology is a radially grown column.

(3) The morphology of the AlN powders is also affected by the diameter of both $AlCl_3$ and NH_3 feeding nozzle, increasing from 6 to 9 mm, and the particle size of resulting powders has a trend of coarsening.

(4) The yield of synthesized AlN powders is affected by the location of the entry/mixing of the reacting $AlCl_3$ and NH_3 gases. The yield increases from 13 to 82% when the mixing location shifts from the front edge to the middle zone of the reactor. In addition, the yield is also affected by the reaction temperature, increasing from 5 to 82%, as the reaction temperature increases from 600° to 1050°C.

3288

References

1. N. S. VANDAMME, S. M. RICHARD and S. R. WINZER, *J. Amer. Ceram. Soc.* **72** (1989) 1409.
2. G. A. SLACK, R. A. TANZILLI, R. O. POHL and J. W. VANDERSANDE, *J. Phys. Chem. Solids* **48** (1987) 641.
3. G. A. SLCCK, *ibid.* **34** (1973) 321.
4. A. A. MOHAMMED and S. J. CORBETT, in Proceeding on the 1985 International Symposium on Microelectronics, Nov. 11–14, 1985, p. 218.
5. A. W. WEIMER, G. A. COCHRAN, G. A. EISMAN, J. P. HENLEY, B. D. HOOK, L. K. MILLS, T. A. GUITON, A. K. KNUDSEN, N. R. NICHOLAS, J. E. VOLMERING and W. G. MOORE, *J. Amer. Ceram. Soc.* **77** (1994) 3.
6. Y. BAIK, K. SHANKER, J. R. MCDERMID and R. A. L. DREW, *ibid.* **77** (1994) 2165.
7. N. KURAMOTO, H. TANIGUCHI and I. ASO, *Amer. Ceram. Soc. Bull.* **68** (1989) 883.
8. T. Z. MORZ, *ibid.* **71** (1982) 782, 784.
9. N. KURAMOTO and H. TANIGUCHI, *J. Mater. Sci. Lett.* **3** (1984) 471.
10. M. M. SEIBOLD and C. RÜSSEL, *J. Amer. Ceram. Soc.* **72** (1989) 1503.
11. F. J. MOURA and R. J. MUNJ, *ibid.* **80** (1997) 2425.
12. K. ISHIZAKI, T. EGASHIRA, K. TANAKA and P. B. CELIS, *J. Mater. Sci.* **24** (1989) 3553.
13. K. BABA, N. SHOHATA and M. YANEZAWA, *Appl. Phys. Lett.* **54** (1989) 2309.
14. M. UDA, W. OHNO and H. OKUYAMA, *Yogyo-Kyokai-Shi* **95** (1987) 76.
15. M. OGAWA and S. ABE, US Patent no. 4610857, 1986.
16. J. R. PARK, S. W. RHEE and K. H. LEE, *J. Mater. Sci.* **28** (1993) 57.
17. I. KIMURA, N. HOTTA, H. NUKUI and N. SAITO, *J. Mater. Sci. Lett.* **7** (1988) 66.
18. R. RIEDEL and K. U. GAUDL, *J. Amer. Ceram. Soc.* **74** (1991) 1331.
19. I. KIMURA, N. HOTTA, H. NUKUI, N. SAITO and S. YASUKAWA, *J. Ceram. Soc. Jpn.* **76** (1988) 206.
20. M. C. WANG, N. C. WU, M. S. TSAI and H. S. LIU, *J. Crystal Growth* **216** (2000) 69.
21. Powder Diffraction Filed Card No. 25-1133, JCPDS Internateral Center for Diffraction Data, Swarthmore, PA, USA, 1975.
22. I. KIMURA, N. HOTTA, H. NUKUI, N. SAITO and S. YASUKAWA, *J. Mater. Sci.* **24** (1989) 4076.
23. T. L. CHU, D. W. ING and A. J. NOREIKA, *Solid-State Electron.* **10** (1967) 1023.
24. K. G. NICKEL, R. RIEDEL and C. PETZOW, *J. Amer. Ceram. Soc.* **72** (1989) 1804.
25. Y. PAULEAU, A. BOUTEVILLE, J. J. HANTZPERGUE, J. C. REMY and A. CACHARD, *J. Electrochem. Soc.* **27** (1980) 1532.
26. M. I. BARATON, X. CHEN and K. E. GONSALVES *J. Mater. Chem.* **6** (1996) 1407.
27. I. C. HUSEBY, *J. Amer. Ceram. Soc.* **66** (1983) 217.